Joint Spatial-Temporal Spectrum Sensing for Cognitive Radio Networks

Tuan Do and Brian L. Mark
Dept. of Electrical and Computer Engineering
George Mason University, MS 1G5
4400 University Drive, Fairfax, VA
email: tdoa@gmu.edu, bmark@gmu.edu

***Abstract*—In a wireless system with opportunistic spectrum sharing, secondary users equipped with cognitive radios attempt to access radio spectrum that is not being used by the primary licensed users. On a given frequency channel, a secondary user can perform spectrum sensing to determine spatial or temporal opportunities for spectrum reuse. Whereas most prior works address either spatial or temporal sensing in isolation, we propose a joint spatial-temporal spectrum sensing scheme, which exploits information from spatial sensing to improve the performance of temporal sensing. Our simulation results show that the proposed joint spatial-temporal approach significantly outperforms existing temporal sensing schemes.**

***Index Terms*—Dynamic spectrum access, cognitive radio, hypothesis testing, spectrum sensing**

I. Introduction

In traditional wireless systems, spectrum or frequency is allocated to licensed users over a geographic area. Within these constraints, spectrum is considered a scarce resource due to static spectrum allocation. Recent empirical studies of radio spectrum usage have shown that licensed spectrum is typically highly under-utilized [1], [2]. To recapture the so-called "spectrum holes," various schemes for allowing unlicensed or secondary users to opportunistically access unused spectrum have been proposed. Opportunistic or dynamic spectrum access is achieved by cognitive radios that are capable of sensing the radio environment for spectrum holes and dynamically tuning to different frequency channels to access them. Such radios are often called *frequency-agile* or *spectrum-agile*.

On a given frequency channel a spectrum hole can be characterized as spatial or temporal. A *spatial* spectrum hole can be specified in terms of the maximum transmission power that a secondary user can employ without causing harmful interference to primary users that are receiving transmissions from another primary user that is transmitting on the given channel. Spectrum reuse in this context is similar to the spectrum reuse that occurs among cochannel cells in a cellular network. A *temporal* spectrum hole is a period of time for which the primary transmitter is idle. During such idle periods, a secondary user may opportunistically transmit on the given channel without causing harmful interference. Most of the prior work on dynamic or opportunistic spectrum access has focused on either spatial or temporal spectrum hole sensing in isolation. In this paper, we propose a joint spatial-temporal sensing scheme and apply it to improve the performance of temporal spectrum sensing.

Spatial spectrum sensing is investigated [3], [4], wherein the maximum interference-free transmit power (MIFTP) of a given secondary user is estimated based on signal strengths received by a group of secondary nodes. To calculate the MIFTP for a secondary node, both the location and transmit power of the primary transmitter are estimated collaboratively by a group of secondary nodes. Using these estimates, each secondary node determines its approximate MIFTP, which bounds the size of its spatial spectrum hole.

In [3], [4], the primary transmitter is assumed to transmit at a constant power. However, this assumption does not allow secondary users to take advantage of temporal spectrum holes. In practice, the primary transmitter may alternate between being active or ON and idle or OFF. To accurately estimate the MIFTP and primary location based on received signal strength, the secondary nodes should determine when the primary transmitter is in the ON and OFF states. When the transmitter is in the ON state, the secondary nodes can employ spatial spectrum sensing to determine the MIFTP.

The problem of detecting when the primary is ON or OFF is called *temporal* spectrum sensing. Temporal cooperative sensing has been studied in [5]–[7]. The decision on the ON/OFF status of the primary transmitter can be made either at individual secondary nodes or collaboratively by a group of secondary nodes. Cooperation among secondary nodes for temporal sensing can overcome problems posed by low signal-to-noise ratio (SNR), shadowing, and hidden terminals [7].

Secondary nodes are generally not aware of the transmission scheme used by the primary transmitter and may not have access to appropriate training signals. For this reason, energy-based detectors are usually preferred to coherent receiver, even though they tend to have poorer performance under low SNR. Both [5] and [6] considered two types of temporal spectrum detection mechanisms: one is based on a joint detection decision made collaboratively by a group of secondary users, while the other is based on a hard decision made at each of the individual secondary nodes. In practice, cooperation is not always possible, especially when cooperating users are far away from each other due to difficulties in gathering all of the received data in a single location.

A practical solution for cooperative temporal sensing is proposed in [7], whereby individual secondary nodes make decisions about the ON/OFF status of the primary transmitter independently. A fusion center or centralized controller collects hard decisions made by all secondary nodes and then make a final decision on whether the primary is idle or busy. In [7], the fusion center is assumed to know the geographic locations of all cooperating secondary nodes and hence can estimate the correlations between their observations. However, the fusion center does not generally have knowledge of the primary's location or transmit power. In [7], a suboptimal temporal detector is proposed based on a linear quadratic (LQ) detector [8], which uses partial statistical knowledge to improve detection performance. The LQ detector outperforms a simpler detector based on a counting rule (CR) in the regime of moderate to high correlation among the secondary nodes.

In this paper[1], we propose a joint spatial-temporal sensing scheme for wireless networks with opportunistic spectrum sharing. During the ON state of the primary transmitter, secondary nodes collaboratively estimate the location and transmit power of the primary transmitter to estimate the MIFTP. Knowledge of the primary's location is used to devise a scheme for temporal spectrum sensing, wherein secondary nodes providing information to the fusion center are chosen intelligently based on their locations relative to the primary transmitter and/or to minimize correlation among the nodes. Our simulation results show that the proposed scheme outperforms CR and LQ detectors that do not exploit spatial information.

The remainder of the paper is organized as follows. Section II describes the system model. Section III discusses a basic framework for temporal spectrum sensing. Section IV proposes a new joint spatial-temporal sensing scheme. Section V presents simulation results. Finally, the paper is concluded in Section VI.

II. System Model

We consider a discrete-time system model with a single primary transmitter and M secondary users equipped with frequency-agile cognitive radios. The primary transmitter can be in one of two states: the ON state, wherein it transmits with constant power s_p, and the OFF state, wherein it does not transmit.

A. Spatial Spectrum Sensing

All transmission are assumed to be omnidirectional and the signal propagation is modeled as a lognormal shadowing model. We follow the path loss model in [9]

$$L = 10n \log_{10}(d/d_0) + L_0 \text{ [dB]}, \tag{1}$$

where d is the distance between transmitting and receiving antennas in meters, L is the path loss in dB, $L_0 \triangleq 20 \log_{10}(\frac{4\pi}{\lambda})$ is the attenuation at distance d_0 in free space, and λ is the wavelength in meters. The free space reference distance d_0 depends on propagation environment. In large coverage cellular systems, a 1 km reference distance may be used, whereas in micro-cellular systems, much smaller distances e.g., 100 m or 1 m are typically used [10].

Accounting for the effect of shadowing and noise, the received power at node v due to node p can be represented as as a lognormal random variable

$$R_v = s_p - 10n \log_{10}(d_{p,v}/d_0) + W \text{ [dBm]}, \tag{2}$$

where n is the path loss factor, s_p is the transmit power of node p at d_0, and $d_{i,j}$ denots the distance between node i and node j in meters. Define the path loss function $g(d) \triangleq 10n \log_{10}(d/d_0)$ and let $L_{i,j} = g(d_{i,j}, n) + W$. We also approximate the sum of the shadowing and noise powers as a lognormally distributed random variable $W \sim \mathcal{N}(0, \sigma_W^2)$, where σ_W^2 is the shadowing noise variance.

We shall make use of some concepts related to spatial spectrum sensing from [3]. The *maximum interference-free transmit power (MIFTP)* of a secondary node is defined as the maximum transmit power on the given channel such that the probability of interference to any potential victim node (i.e., a primary receiver) is less than a prescribed threshold. The *outage probability* of a victim node v with respect to the transmitter p, is the probability that the received power R_v from node p below a predetermined detection threshold $r_{\min}$:

$$P_{\text{out}}(p, v) \triangleq P(R_v < R_{\min}).$$

The *coverage distance* is the maximum distance between node p and any potential victim node v such that P_{out} does not exceed a predefined threshold $\epsilon_{\text{cov}} > 0$:

$$d_{\text{cov}}(p) \triangleq \max\{d_{p,v} : P_{\text{out}}(p, v) \leq \epsilon_{\text{cov}}\}.$$

The *coverage region* of the transmitter p is the closed disk centered at node p with radius $d_{\text{cov}}(p)$. The received power at node v from node a is given by

$$I_v = s_a - g(d_{a,v}) + W,$$

where s_a is the transmit power of a.

The *interference probability* in the spatial domain with respect to a given victim node v is the probability that I_v exceeds a predefined interference tolerance threshold $i_{\max}$: $P_s(a, v) \triangleq P(I_v \geq i_{\max})$. For a fixed primary transmitter p and FAR node a, the MIFTP is the maximum transmit power of the FAR node such that the interference probability with respect to any potential victim node within the coverage distance from node p does not exceed a threshold $\epsilon_{\text{int}} > 0$:

$$s_a^* \triangleq \max\{s_a : P_s(a, v) \leq \epsilon_{\text{int}}, \forall v : d_{p,v} \leq d_{\text{cov}}(p)\}.$$

The worst case interference probability is given by

$$P_s(a) = \sup_v P_s(a, v) = Q\left(\frac{i_{\max} - s_a + g(d_a^*)}{\sigma_W}\right), \tag{3}$$

[1]This work was supported in part by the U.S. National Science Foundation under Grants CNS-0520151 and ECS-0246925.

where $d_a^* \triangleq d_{p,a} - d_{\mathrm{cov}}(p)$. Therefore the MIFTP can be expressed as

$$s_a^* = \max\{s_a : P_s(a) \le \epsilon_s\} \quad (4)$$
$$= \begin{cases} i_{\max} + g(d_a^*) - \sigma_w Q^{-1}(\epsilon_{\mathrm{int}}), & d_{p,a} > d_{\mathrm{cov}}(p), \\ -\infty & \text{otherwise.} \end{cases} \quad (5)$$

To mitigate the effect of shadowing and low SNR, cooperation among the secondary nodes is necessary to perform both spatial and temporal spectrum sensing. The detection distance is the distance from the primary transmitter beyond which a secondary node cannot detect the primary signal and is given by [3]

$$d_{\mathrm{det}}(a) = g^{-1}(s_p - r_a + \sigma_W Q^{-1}(1 - \epsilon_{\mathrm{cov}})),$$

where g^{-1} is the inverse function of g and r_a is the detection threshold of the FAR nodes. We assume that all secondary nodes have the same detection distance, i.e., they are equipped with detectors having the same receiver sensitivity. The set of secondary nodes that perform temporal sensing may be different from the set of nodes that perform spatial sensing. Let $\mathcal{S}$ and $\mathcal{T}$ denote the set of nodes that are involved in spatial sensing and temporal sensing, respectively. The nodes in $\mathcal{S}$ are located within a disk centered at primary transmitter location (x_p, y_p) and radius equal to detection distance $d_{\mathrm{det}}(a)$.

III. Temporal Spectrum Sensing

A. Temporal Sensing Model

We adopt a model of temporal spectrum sensing similar to the one described in [7]. Each secondary node involved in temporal sensing (i.e., in the set $\mathcal{T}$) makes an independent decision about the ON/OFF state of the primary transmitter. All local decisions from nodes in $\mathcal{T}$ are then communicated to a centralized controller or fusion center, where the final decision about the state of the primary transmitter is made. Alternatively, the system could distributed, such that the secondary nodes exchange their local decisions and each of them performs its own fusion of all decisions. For concreteness, we shall assume the simpler centralized model in the following discussion.

By communicating with the secondary nodes in $\mathcal{T}$, the fusion center obtains estimates of the geographic locations of all secondary nodes and the location of the primary transmitter. The main task of the fusion center is to decide whether the primary transmitter is in the ON or OFF state. We assume that all secondary nodes use identical energy detectors. Since the nodes in $\mathcal{T}$ are expected to be located relatively close to each other, the received powers at these nodes are assumed to be identically distributed and correlated.

Temporal spectrum sensing can be formulated as a binary hypothesis testing problem in which the fusion center determines whether or not the current mean received power is higher than the received power when the primary transmitter is in the OFF state [7]. When the primary transmitter is OFF, the power at the output of energy detector becomes the sum of the noise power and the power of interfering signals. Both of these power components can be measured at the secondary nodes, but due to variations in the noise level at the receivers, perfect knowledge of the noise powers cannot be obtained. We model the uncertainty using a lognormal distributed distribution [11] and assume that the noise powers are independent and identically distributed across the secondary nodes.

We define two hypotheses: H_1 is the hypothesis that the primary is ON and located close to the secondary nodes and H_0 is the hypothesis that the primary is OFF or far away. In other words, H_0 is the hypothesis that the temporal spectral hole exists and the frequency channel is available for reuse by secondary users. Node $i \in \mathcal{T}$ performs temporal sensing by computing an observation Y_i, obtained by subtracting an estimate of the sum of the noise and interference power from the received power. Let $\mathbf{Y} = (Y_i : i \in \mathcal{T})$ represent the vector of observations at a given observation epoch.

The hypothesis testing problem can then be formulated as follows:

$$H_0 : \mathbf{Y} \sim \mathcal{N}(\mathbf{0}, \sigma_0^2 \mathbf{I}) \quad (6)$$
$$H_1 : \mathbf{Y} \sim \mathcal{N}(\alpha \mathbf{1}, \mathbf{\Sigma}), \quad (7)$$

with $\alpha \ge \mu$, where

$$\mu \triangleq E[10 \log_{10}(1 + \gamma_{\min})] \text{ [dB]},$$

and $\gamma_{\min}$ is the signal-to-noise ratio (SNR) at the secondary nodes at the largest distance to primary user or, equivalently, the smallest mean received SNR when the primary is ON. In (7), $\mathcal{N}(\mathbf{v}, \mathbf{\Sigma})$ denotes the multivariate Gaussian vector distribution with mean $\mathbf{v}$ and covariance matrix $\mathbf{\Sigma}$ and σ_0^2 is the variance of the noise power. The symbols $\mathbf{0}$ and $\mathbf{1}$ denote the vectors of all zeros and ones, respectively, and $\mathbf{I}$ denotes identity matrix. The (i,j) element of the covariance matrix $\mathbf{\Sigma}$ is given by $\Sigma_{ij} = \sigma_1^2 \rho^{d_{ij}/D_c}$ where d_{ij} is the distance between nodes i and j in meters and ρ is the correlation coefficient between secondary nodes separated by correlation distance D_c in meters. The parameter α represents the mean power of the distributions observed under hypothesis H_1.

The temporal sensing system is designed such that the probability of interference with the primary transmitter is less than or equal to a pre-specified value P_t:

$$P(\delta = H_0 | H_1) \le P_t, \quad (8)$$

where δ is the decision rule determined by the fusion center. In general, the temporal sensing interference probability P_t does not necessarily equal the spatial sensing interference probability P_s given in (3). The constraint (8) must be satisfied for all values of $\alpha \ge \mu$ in (7). Since the prior information about the distribution of the mean power α is unknown, the composite binary hypothesis testing problem (7) is designed under a robust and universally most powerful detection framework [12]. In other words, the system is designed such that (8) is satisfied for the least favorable value of α, i.e., $\alpha = \mu$ [7]. This results in a simple Neyman-Pearson hypothesis testing problem:

$$H_0 : \mathbf{Y} \sim \mathcal{N}(\mathbf{0}, \sigma_0^2 \mathbf{I}),$$
$$H_1 : \mathbf{Y} \sim \mathcal{N}(\mu \mathbf{1}, \mathbf{\Sigma}). \quad (9)$$

The final decision δ is made at the fusion center, which has access to only binary-value decisions made individually by the secondary nodes based on the observation $\{Y_i : i \in \mathcal{T}\}$. We denote by U_i the individual decision made by the ith temporally sensing secondary node, based on the observation Y_i. Correspondingly, $\mathbf{U} = (U_i : i \in \mathcal{T})$ denotes the vector of individual decisions to represent vector of decisions made by the secondary nodes.

B. Temporal Sensing Detection Rules

Let

$$L(Y_i) \triangleq \frac{p_1(Y_i)}{p_0(Y_i)},$$

denote the likelihood ratio of the observation at node $i \in \mathcal{T}$, where $p_0(\cdot)$ and $p_1(\cdot)$ denote, respectively, the posterior distributions under hypotheses H_0 and H_1, respectively. Then the optimal decision at node i can be represented as

$$U_i = I_{\{\ln L(Y_i) > \tau\}},$$

where I_A denotes the indicator function of the set A the threshold τ is chosen to ensure that (8) is satisfied. The fusion center makes a final decision on the decision bit vector $\mathbf{U}$.

Under the so-called *counting rule (CR)*, the final decision is made by comparing the sum $\sum_{i \in \mathcal{T}} U_i$ to a decision threshold. The value of this threshold is obtained through simulation [7]. When the observations across all of the nodes are independent, identical distributed under both hypotheses, the CR detector is optimal, since the joint likelihood ratio of the bits is a function of only the type of the received bit vector $\mathbf{U}$. The CR detector is efficient when the correlations between the individual observations Y_i are small.

When the observations at the secondary nodes are correlated, the Linear Quadratic (LQ) detector yields a significant performance gain over the CR detector, while still using only partial statistical knowledge about the correlated decision variables [7]. The LQ detector is based on the *generalized signal-to-noise ratio* or deflection criterion, and makes use of fourth-order statistics under H_0 and second order statistics under H_1 (see [7] for details).

IV. Joint Spatial-Temporal Sensing

In this section, we propose a new joint spatial-temporal sensing technique for spectrum hole discovery in cognitive radio networks. The basic idea is to make the temporal sensing decision based on the individual decisions of a subset $\tilde{\mathcal{T}}$, of $\mathcal{T}$, which is selected intelligently based on knowledge of the spatial location and transmit power of the primary transmitter obtained through spatial sensing. The secondary nodes collaboratively decide whether the primary is in the ON or OFF state. If the primary is determined to be ON, the secondary nodes collaboratively estimate the location and transmit power of the primary transmitter. Each of the secondary nodes can then compute its MIFTP. When the primary transmitter is determined to be ON, one of the secondary nodes may transmit with power up to its estimated MIFTP value. Otherwise, when the primary is determined to be OFF, one of the secondary nodes may transmit with up to some maximum power level P_m. The secondary node that is allowed to transmit is determined through collaboration among the secondary nodes via a networking protocol.

Based on the estimates of the primary's location and transmit power, as well as knowledge of the secondary node locations and correlations between the nodes, the fusion center fuses the individual decisions from the "best" subset of T nodes from the set $\mathcal{T}$ based on one of two criteria:

1) minimum distance to the primary user;
2) minimum correlations between secondary nodes.

When the correlation between secondary nodes is small and all secondary nodes have the same received SNR, the CR detector outperforms the LQ detector [7]. In this case, use of criterion 2 results in better performance than use of criterion 1. However, when the received SNRs are different among the nodes, use of criterion 1 achieves better performance. Our overall conclusion is that intelligent selection of nodes based on spatial knowledge can significantly improve the performance of temporal sensing.

We propose a suboptimal, but simple heuristic that attempts to select a subset of nodes to minimize the correlation between the nodes in this subset, in accordance with criterion 2. Assume that $|\mathcal{T}| > T$. The heuristic initializes $\tilde{\mathcal{T}} \leftarrow \mathcal{T}$ and then proceeds as follows:

H1. Let $(a, b) = \arg\min_{i,j \in \tilde{\mathcal{T}}} d_{i,j}$.
H2. If $d_{a,p} < d_{j,p}$, then $\tilde{\mathcal{T}} \leftarrow \tilde{\mathcal{T}} - \{a\}$; else, $\tilde{\mathcal{T}} \leftarrow \mathcal{S} - \{b\}$.
H3. If $|\tilde{\mathcal{T}}| = T$ stop; else, go to H1.

V. Numerical Results

In this section, we compare the performance of the proposed joint spatial-temporal sensing scheme with other pure temporal sensing schemes in two different scenarios. In both cases, we assume that the transmit power, s_p, of the primary transmitter is unknown. Under joint spatial-temporal sensing, the secondary nodes collaboratively estimate both s_p and the location of the primary. The following parameters are used in all simulations:

- Detection threshold $r_{\min} = -30$ dBm;
- $i_{\max} = -80$ dBm, $\epsilon_{\text{int}} = 0.01$ and $\epsilon_{\text{cov}} = 0.05$;
- Standard deviation of shadowing noise, $\sigma_W = 4$ dB;
- primary location $L_p = (5000, 5000)$ [m];
- $s_p = 80$ dBm;
- path loss factor $n = 3$
- $\sigma_0 = 1$ dB, $\sigma_1 = 2.1$ dB;
- Mean total power $\mu = 3.4$ dB.

As shown in Fig. 1, the locations of $|\mathcal{S}| = 20$ secondary nodes for spatial spectrum sensing are generated randomly with uniform distribution in the disk centered at L_p with radius equal to $d_{\text{det}}(a)$. All temporal sensing nodes are placed

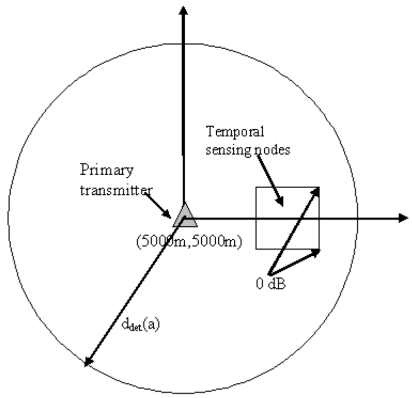

Fig. 1. Generation of secondary node locations.

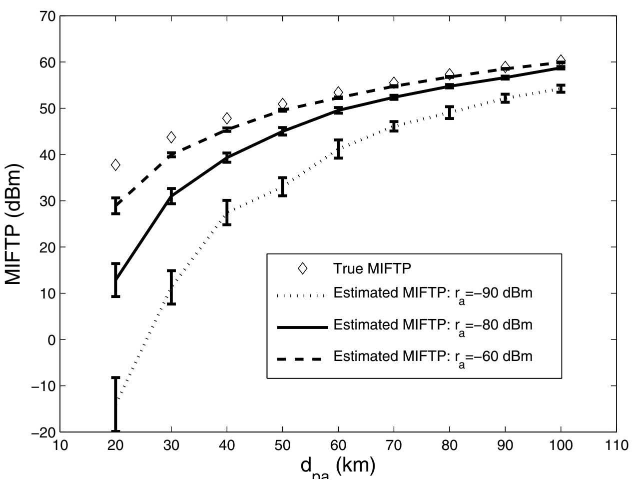

Fig. 2. Estimated MIFTP over different r_a.

inside a square with the smallest possible mean received SNR $\gamma_{\min} = 0$ dB.

Scenario 1

The suburban environment correlation model in [13] is assumed, with $d_0 = 1$ m, correlation coefficient $\rho = 0.6$, and correlation distance $D_c = 250$ m. We place 18 temporal sensing nodes inside the square area indicated in Fig. 1 with edge length equal to $D_c/2 = 125$ m. Out of the 18 nodes, nine are distributed uniformly over the coverage area, while the remaining nine are distributed uniformly inside the square. Because the nodes inside the square have different SNRs and the correlation ρ is relatively large, the fusion center chooses the decisions from the nine nodes closest to the primary transmitter based on its estimated location. Fig. 2, shows the values of MIFTP estimated with different r_a as a function of the distance d_{pa} to the primary transmitter. The primary transmitter location, transmit power, and the MIFTP are all estimated by the secondary nodes in $\mathcal{S}$, which participate in spatial spectrum sensing.

Fig. 3 compares the performance of various temporal spectrum sensing schemes in this scenario. The vertical axis is

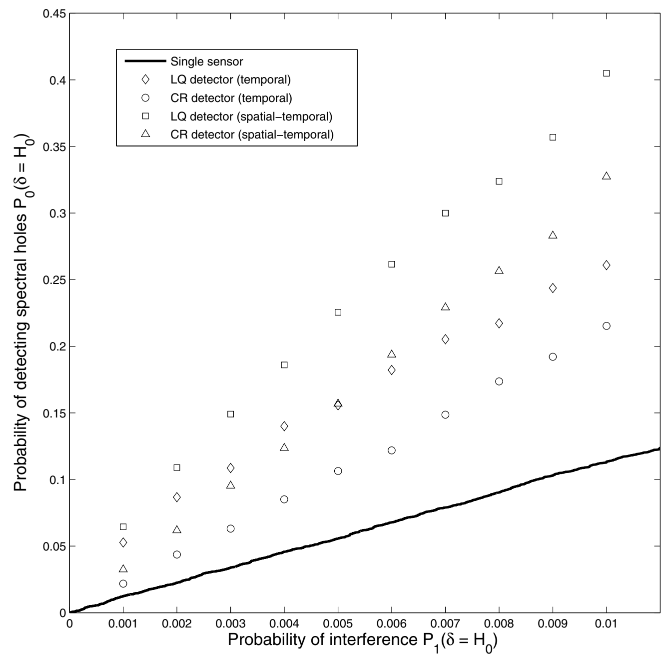

Fig. 3. Spatial-temporal sensing vs. temporal sensing with $\rho = 0.6$.

the probability of detecting a spectrum hole, $P_0(\delta = H_0)$, while the horizontal axis shows the probability of interference, $P_1(\delta = H_0)$. As a baseline, the performance of a single sensor is shown as the solid line. The other performance curves are obtained using collaborative temporal sensing. The performance curves for pure temporal sensing under the counting rule (CR) and the linear quadratic (LQ) detector are shown with circles and diamonds, respectively. The LQ detector is seen to clearly outperform CR, which confirms the results in [7].

Performance curves for joint spatial-temporal sensing using the CR and LQ detectors are shown with triangles and squares, respectively. Spatial-temporal sensing is performed using criterion 1 (see Section IV). We see that the spatial-temporal LQ detector has the best performance over all values of $P_1(\delta = H_0)$. We also observe that the spatial-temporal CR detector performs worse than the temporal LQ detectors when $P_1(\delta = H_0)$ is small and better when $P_1(\delta = H_0)$; the crossover point is approximately 0.005. Fig. 3 clearly shows the benefit of incorporating spatial information into temporal spectrum sensing.

Scenario 2

In the second simulation scenario, we set $d_0 = 100$ m, $\rho = 0.3$, correlation distance $D_c = 300$ m. All nodes in $\mathcal{T}$ have almost the same received SNR. In this scenario, we have $|\mathcal{T}| = 18$ total nodes for temporal sensing, which are located randomly in the square shown in Fig. 1 according to a uniform distribution. A subset, $\tilde{\mathcal{T}}$ of $T = 9$ nodes is chosen from the original set $\mathcal{T}$ according to one of the two criteria discussed in Section IV. Fig. 4 compares the performance of the following four spatial-temporal detectors:

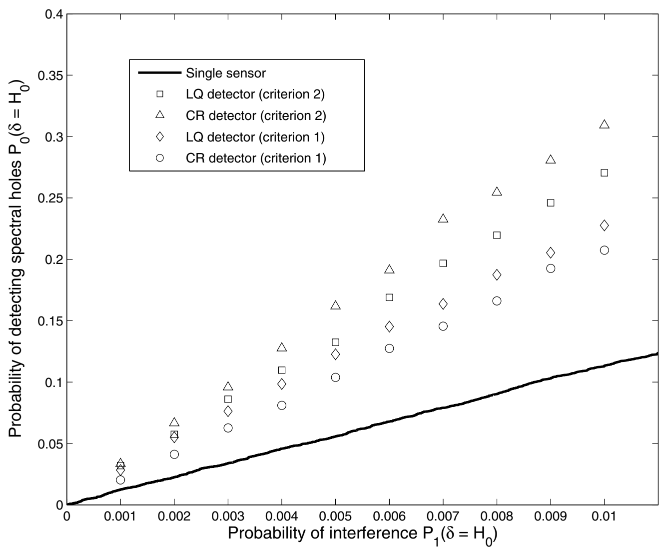

Fig. 4. Joint spatial-temporal sensing with different node selection criteria and $\rho = 0.3$

1) LQ detector under criterion 1;
2) CR detector under criterion 1;
3) LQ detector under criterion 2;
4) CR detector under criterion 2.

In this scenario, the heuristic given in Section IV is used to implement criterion 2 approximately. From Fig. 4, we observe that when the correlation is small and the received SNRs are similar, better performance is achieved with criterion 2, i.e., the nodes are selected to minimize the correlation. Under criterion 2, the CR detector outperforms the LQ detector because criterion 2 minimizes the correlation among the observations, and when the correlation is small, the CR detector outperforms the LQ detector according to [7]. However, under criterion 1, the LQ detector still outperforms the CR detector because the correlation remains relatively high.

VI. Conclusion

We proposed a joint spatial-temporal sensing scheme for opportunistic spectrum sharing in cognitive radio networks. The system model consists of a primary transmitter with unknown location and transmit power, which alternates between ON and OFF states, with respect to a given frequency channel. Spatial spectrum sensing is employed to estimate the maximum interference transmit power for a secondary node during an ON period. Estimates of the primary transmitter's location and transmit power obtained in the course of spatial sensing are used by a fusion center to select a subset of the secondary nodes to make a temporal sensing decision, i.e., a decision as to whether the primary is ON or OFF. Two distributed temporal sensing algorithms are considered: the counting rule detector and the linear quadratic detector. By incorporating spatial information, we developed joint spatial-temporal versions of these two detectors.

Our simulation results show that joint spatial-temporal sensing approach significantly outperform pure temporal sensing, in terms of probability of spectrum hole detection. In this paper, we assumed only a single primary transmitter on a given frequency channel. In ongoing work, we are investigating joint spatial-temporal sensing in the presence of multiple cochannel transmitters.

References

[1] M. McHenry, "Frequency agile spectrum access technologies," in *FCC Workshop on Cognitive Radio*, May 2003.
[2] R. W. Broderson, A. Wolisz, D. Cabric, S. M. Mishra, and D. Willkomm, "CORVUS: A Cognitive Radio Approach for Usage of Virtual Unlicensed Spectrum," White Paper, Univ. California Berkeley, Tech. Rep., July 2004.
[3] B. L. Mark and A. O. Nasif, "Estimation of maximum interference-free transmit power level for opportunistic spectrum access," *IEEE Trans. on Wireless Commun.*, 2009 (to appear).
[4] ——, "Estimation of interference-free transmit power for opportunistic spectrum access," in *Proc. IEEE WCNC'08*, Las Vegas, NV, Apr. 2008.
[5] S. M. Mishra, A. Sahai, and R. W. Brodersen, "Cooperative sensing among cognitive radios," in *Proc. IEEE ICC'06*, vol. 4, Istanbul, June 2006, pp. 1658–1663.
[6] E. Visotsky, S. Kuffner, and R. Peterson, "On collaborative detection of tv transmissions in support of dynamic spectrum sharing," in *Proc. IEEE DySPAN'05*, Nov. 2005, pp. 338–345.
[7] J. Unnikrishnan and V. Veeravalli, "Cooperative sensing for primary detection in cognitive radio," *IEEE J. Sel. Topics Signal Process.*, vol. 2, no. 1, pp. 18–27, Feb. 2008.
[8] B. Picinbono and P. Duvaut, "Optimal linear-quadratic systems for detection and estimation," *IEEE Trans. Inf. Theory*, vol. 34, no. 2, pp. 304–311, 1988.
[9] C. Perez-Vega and J. M. Zamanillo, "Path-loss model for broadcasting applications and outdoor communication systems in the VHF and UHF bands," *IEEE Trans. Broadcasting*, vol. 48, no. 2, pp. 91–96, Jun. 2002.
[10] T. S. Rappaport, *Wireless Communication: Principles and Practice*, 2nd ed. Englewood Cliffs, NJ: Prentice-Hall, 2001.
[11] K. V. Cai, V. Phan, and R. J. O'Connor, "Energy detector performance in a noise fluctuating channel," in *Proc. IEEE Milcom'89*, 1989, pp. 85–89.
[12] H. V. Poor, *An Introduction to Signal Detection and Estimation*, 2nd ed. NewYork, NY: Springer-Verlag, 1994.
[13] M. Gudmundson, "Correlation model for shadow fading in mobile radio systems," *IEEE Electron. Lett.*, vol. 27, no. 23, pp. 2145–2146, Nov. 1991.